C. R. Chimie 19 (2016) 371–380

Contents lists available at ScienceDirect

Comptes Rendus Chimie

www.sciencedirect.com

Full paper/Mémoire

Manganese(III) porphyrin supported onto multi-walled carbon nanotubes for heterogeneous oxidation of synthetic textile dyes and 2,6-dimethylphenol by *tert*-butyl hydroperoxide

Saeed Rayati*, Zahra Sheybanifard

Department of Chemistry, K.N. Toosi University of Technology, P.O. Box 16315-1618, 15418 Tehran, Iran

ARTICLE INFO

Article history:
Received 1 July 2015
Accepted 3 December 2015
Available online 21 January 2016

Keywords:
Heterogeneous oxidation
Mn-porphyrin
Carbon nanotubes
Textile dyes
2,6-Dimethylphenol

ABSTRACT

Manganese porphyrin has been supported onto multi-walled carbon nanotubes (Mn(TCPP)OAc@MWCNT) and characterized by powder X-ray diffraction, FT-IR, atomic absorption and UV–vis spectroscopy, field emission scanning electron microscopy (FE-SEM) and also thermogravimetric analysis (TGA). The TGA curve shows that the nanocatalyst was thermally stable up to almost 350 °C. This catalyst was found to be able to oxidize different synthetic textile dyes in aqueous media over a wide pH range at ambient temperature with *tert*-butyl hydroperoxide (TBHP) as the oxygen source. The influence of some important parameters such as the initial pH of the dye solution, temperature and concentration of the catalyst, the oxidant and the co-catalyst were investigated. Also, the ability of this heterogeneous catalyst to oxidize 2,6-dimethylphenol (with excellent selectivity for quinone (86%)) with TBHP in acetonitrile was evaluated. The separation and recycling of the catalyst is simple and the catalyst can be used several successive cycles without significant decrease in catalytic activity.

1. Introduction

In recent decades, increasing productions in the chemical industry has led to the making of millions of tons of unwanted compounds which are often harmful from an environmental point of view. Thus, the degradation and elimination of these compounds has been subject of extensive academic research. Synthetic textile dyes and industrial pigments are essential chemicals which are used extensively in industries such as textiles, papers, leathers, cosmetics, food and additives [1,2]. Textile and dyeing industries produce a large quantity of coloured waste compounds and thus, the removal of coloured waste from industrial wastewater is imperative. Although substantial efforts have been made and numerous methods have been utilized, the problem remains unsolved [3–4]. Recently, catalytic oxidation processes have been widely used for the transformation of the pollutants into more functional and non-toxic compounds [5–13]. Among different catalytic systems, synthetic metalloporphyrin complexes have been extensively examined as models of cytochrome P-450 over the last few decades [14–18].

Homogeneous metalloporphyrin catalytic systems are very effective in catalytic oxidation reactions but problems such as oxidative degradation of porphyrin and the impossibility of separating the products and recovering the catalyst have led to the scarce use of these complexes. Studies have indicated that the use of solids as supports for the immobilization of metalloporphyrin complexes can be a suitable way of improving their efficiency and stability [19–22]. Among the various possible solid supports, carbon

* Corresponding author.
E-mail addresses: rayati@kntu.ac.ir, srayati@yahoo.com (S. Rayati).

http://dx.doi.org/10.1016/j.crci.2015.12.001
1631-0748/

nanotubes can be a good choice due to their unique properties such as structural characteristics, high surface area and the lack of solubility in most solvents [23,24]. We have reported the ability of supported Mn- and Fe-porphyrins in the oxidation of alkenes with *tert*-butyl hydroperoxide (TBHP) and H_2O_2 [25–28]. In the present research, a heterogeneous catalyst was prepared by covalent bonding between Mn(TCPP)OAc and functionalized carbon nanotubes and its catalytic efficiency was examined for oxidative degradation of different synthetic textile dyes using TBHP in aqueous media.

Other hazardous materials are phenolic compounds which are inexpensive and readily available and have been used in petrochemical and pharmaceutical industries [29,30]. Oxidation reactions can be a suitable way for removing these compounds and turning them into more beneficial compounds such as quinones which are prominent intermediates in organic syntheses [31–33]. In general, in comparison with other compounds such as hydrocarbons and sulfides, metalloporphyrins are less frequently considered in the oxidation of phenolic compounds. Hence, we checked the ability of this catalytic system for the oxidation of 2,6-dimethylphenol in acetonitrile.

2. Experimental section

2.1. Materials

Functionalized multi-walled carbon nanotubes containing 3.06 wt% hydroxyl groups with an outside diameter of 10–20 nm, inside diameter of 5–10 nm, length of ~30 μm and specific surface area of >200 m^2/g were used as the solid support. Other materials and solvents were purchased from Merck or Fluka chemical companies and used as received. Distilled water was utilized throughout the dye oxidative degradation processes.

2.2. Physico-chemical characterization techniques

Field emission scanning electron microscopy (FE-SEM) images were obtained on a Hitachi S-4160 with an accelerating voltage of 20 kV. Thermogravimetric analysis (TGA) was carried out with a Mettler-Toledo TGA 851e apparatus at a heating rate of 10 K min^{-1} in a nitrogen atmosphere. FT-IR spectra were recorded on an ABB Bomem: FTLA 2000-100 in the range of 400–4000 cm^{-1} using KBr pellets. A Varian AA240 atomic absorption spectrometer was utilized to determine the amount of Mn-porphyrin complex absorbed onto the solid support. The electronic spectra were taken on a single beam spectrophotometer (Cam Spec-M330 model) in a 2 mm path length quartz cell in the range of 200–800 nm. For adjusting the pH values of the dye solution a PHS-3C pH meter was utilized. A Bruker FT-NMR 500 (500 MHz) spectrometer was utilized to record ^1H NMR spectra in $CDCl_3$ solution. The powder XRD patterns were recorded using an STOE STADIP diffractometer equipped with a scintillation detector, secondary monochromator and Cu-Kα1 radiation (λ = 1.5406 Å). In order to reveal the reaction products arising from the oxidative degradation of dyes, high-performance liquid chromatography mass spectrometry (HPLC-MS) (Agilent 6410) was used which was equipped with a Agilent Zorbox C8 column (4.6 mm × 150 mm, 5 μm) and whose mobile phase was composed of 0.01 mol/L of acetonitrile-ammonium acetate (30/70, v/v) solution (pH = 6.8) and also, 20 μL of sample was injected by an autosampling device. The eluent from the chromatographic column sequentially entered the UV–vis diode array detector. The mass spectrometer was equipped with an electrospray ionization (ESI) source and operated in negative ion mode. Oxidation of 2,6-dimethylphenol was monitored by gas chromatography (Shimadzu GC-14B) equipped with a flame ionization detector (FID) with a SAB-5 capillary column (phenyl methyl siloxane 30 m × 320 mm × 0.25 mm). In the GC experiments, n-octane was used as an internal standard.

2.3. Catalyst preparation ((Mn(TCPP)OAc) and its supported form (Mn(TCPP)OAc@MWCNT))

Meso-tetrakis(4-carboxyphenyl)porphyrin (H_2TCPP) and *meso*-tetrakis-(4-carboxyphenyl)porphyrinatomanganese-(III) acetate (Mn(TCPP)OAc) were prepared according to methods described in the literature studies [34,35]. The Mn(III) porphyrin complex was anchored covalently onto the functionalized multi-walled carbon nanotubes by the following procedure: to a mixture of 500 mg of MWCNT-OH in 50 mL DMF, 360 mg of Mn(TCPP)OAc, 400 mg of 2-(1*H*-benzotriazole-1-yl)-1,1,3,3-tetramethyluronium tetrafluoroborate (TBTU) and 300 mg of *N,N′*-diisopropylamine (DIPEA) were added and the mixture was stirred for 48 h at room temperature. The dark solid product was filtered and washed several times with DMF for removing the weakly adsorbed metalloporphyrins and was eventually dried at room temperature [26,36].

2.4. Catalytic oxidative degradation of the synthetic textile dyes

The catalytic reactions were run in 5 mL test tubes or 10 mL glass flasks in a water bath. To a 500 mg/dm^3 aqueous solution of dye (3.3 cm^3 of methyl orange (MO), 3.2 cm^3 of methylene blue (MB), 4 cm^3 of crystal violet (CV) and 6.9 cm^3 of congo red (CR) that are equal to 5×10^{-6} mol), 1 mg of the catalyst and 9×10^{-3} cm^3 of TBHP as the oxidant were added. Also, various amounts of imidazole as the co-catalyst have been used. The solution pH was adjusted with ammonium acetate buffer solutions (0.01 M). To monitor the oxidative degradation process, solution samples were taken out at given time intervals and measured by UV–vis spectroscopy and the calibration curve using the characteristic band of each dye (MO: 464 nm, CR: 498, MB: 660 nm, and CV: 590 nm).

2.5. Oxidation of 2,6-dimethylphenol

0.06 mmol of 2,6-dimethylphenol in 0.5-mL acetonitrile, 1.7 mg imidazole as the co-catalyst and 2.5 mg of the supported catalyst have been added in a 5 mL test tube. The oxidation reaction was run at ambient temperature after adding 23 μL of TBHP to the reaction mixture. The progress of the reaction was monitored by GC. After the completion of the reaction, the reaction mixture was centrifuged to

separate the catalyst. Oxidation products were separated on pre-coated F254 silica gel plates (Merck), 2 mm thickness, and 20 × 20 cm, using *n*-hexane/ethyl acetate (0.1: 0.9) as the eluent and were identified using ^{1}H NMR by comparison with authentic samples.

3. Results and discussion

3.1. Characterization of the supported catalyst (Mn(TCPP)OAc@MWCNT)

Mn-porphyrin has been covalently anchored onto the functionalized multi-walled carbon nanotubes using TBTU as an impressive coupling reagent for esterification in the presence of DIPEA as a base. The proposed structure of the supported catalyst is presented in Fig. 1.

The covalent bonding of the supported catalyst was investigated by comparison of the FT-IR spectra of Mn(TCPP)OAc and Mn(TCPP)OAc@MWCNT (Fig. 2). The peaks at 1649.62 cm^{-1} and 1652.11 cm^{-1} in the FT-IR spectra of the Mn-porphyrin and supported catalyst were attributed to the stretching vibrations of the phenyl rings in the *meso* positions of the porphyrin molecule [37]. The sharp peak at 1724.51 cm^{-1} was ascribed to the esteric linkage between Mn-porphyrin and MWCNT-OH (Fig. 2b). The most informative spectroscopic data, regarding the covalent bonding of Mn(TCPP)OAc onto MWCNT-OH, were obtained by comparison of the UV–vis spectra of Mn(TCPP)OAc, MWCNT-OH and Mn(TCPP)OAc@MWCNT (Fig. 3). The absorption spectrum of Mn(TCPP)OAc in DMF exhibits a sharp peak at 470 nm (Soret bond) and two weak absorptions at 566 nm and 601 nm (Q bonds) as shown in Fig. 3a. The UV–vis spectrum of MWCNT-OH and Mn(TCPP)OAc@MWCNT confirmed that the bands detected in Fig. 3b are due to the Mn-porphyrin, because the UV–vis spectrum of MWCNT-OH does not exhibit any bands in the target region.

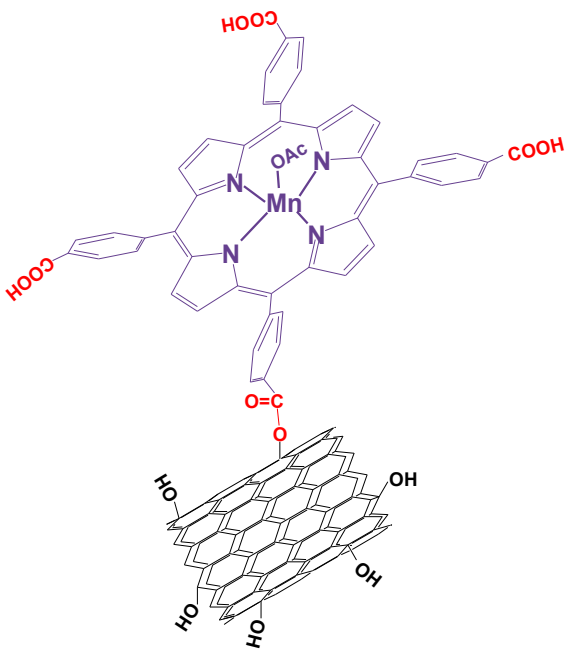

Fig. 1. Schematic representation of the 5, 10, 15, 20-tetrakis(4-carboxyphenyl) porphyrinatomanganese(III) acetate supported onto the surface of functionalized multi-walled carbon nanotubes (Mn(TCPP)OAc@MWCNT).

After anchoring the metalloporphyrin, the Soret band (474 nm) shows a red-shift (4 nm) in comparison with the metalloporphyrin in solution. The steric constraints of the support which caused a modification of the metalloporphyrin can be an explanation for this behaviour [12,38–40].

Atomic absorption spectroscopy exhibited that the metal content of the supported catalyst was 497.4 μmol per gram catalyst. This amount is higher than other immobilization approaches in the literature studies [37,41] which may be due to the use of a very effective uronium salt as a coupling reagent.

The morphology of the prepared catalyst indicates that carbon nanotubes are aggregated and their nanotube nature has been kept after anchoring the metalloporphyrin complexes to them (Fig. 4). These results are in agreement with those obtained by other studies [25,41].

Fig. 5 shows the X-ray diffraction patterns of MWCNT and Mn(TCPP)OAc@MWCNT in the range of $2\theta = 10°–90°$. The diffraction peaks on the 2θ values of 25.5°, 42° and 44° which are related to the (002), (100) and (101) planes, respectively, are characteristic diffraction peaks of carbon nanotubes (Fig. 5b). The similarity of the XRD pattern before and after supporting onto nanotubes confirms that the Mn-porphyrin complex was dispersed onto MWCNTs and also the nature of the MWCNTs has been preserved [37,42].

Thermogravimetric analysis of Mn(TCPP)OAc@MWCNT is illustrated in Fig. 6a. A comparison with the Mn(TCPP)OAc (Fig. 6b) shows that the heterogeneous catalyst is thermally stable up to 350 °C. The mass loss below 300 °C corresponds to the loss of humidity [28]. The mass decline around 350–700 °C may be due to the decomposition of Mn(TCPP)OAc followed by the oxidation of MWCNTs [37].

3.2. Catalytic oxidative degradation of the synthetic textile dyes

The synthesized heterogeneous catalyst was utilized for the catalytic oxidative degradation of methyl orange (MO) as a model which is often used in analytical chemistry as an acid-base indicator. The UV–vis spectrum of this compound in water displays two peaks at 270 nm and 464 nm, the latter of which attributed to the n→л* transition of the N=N group [43]. The influence of different parameters including pH, presence of imidazole as the axial base, reaction time, temperature, and amount of catalyst and oxidant were evaluated by changing one parameter while the others were kept constant.

There is minor oxidation in the absence of either the catalyst or the TBHP (Table 1, entries 1 and 2). In addition, the adsorption of methyl orange onto the MWCNT-OH was very low (Table 1, entry 3). Catalytic activity of Mn-porphyrins has been usually affected by the presence of nitrogenous bases [44,45]. Thereby, the effect of imidazole as a co-catalyst on the oxidation of MO has been tested (Table 1, entries 4–10). According to the results, the use of

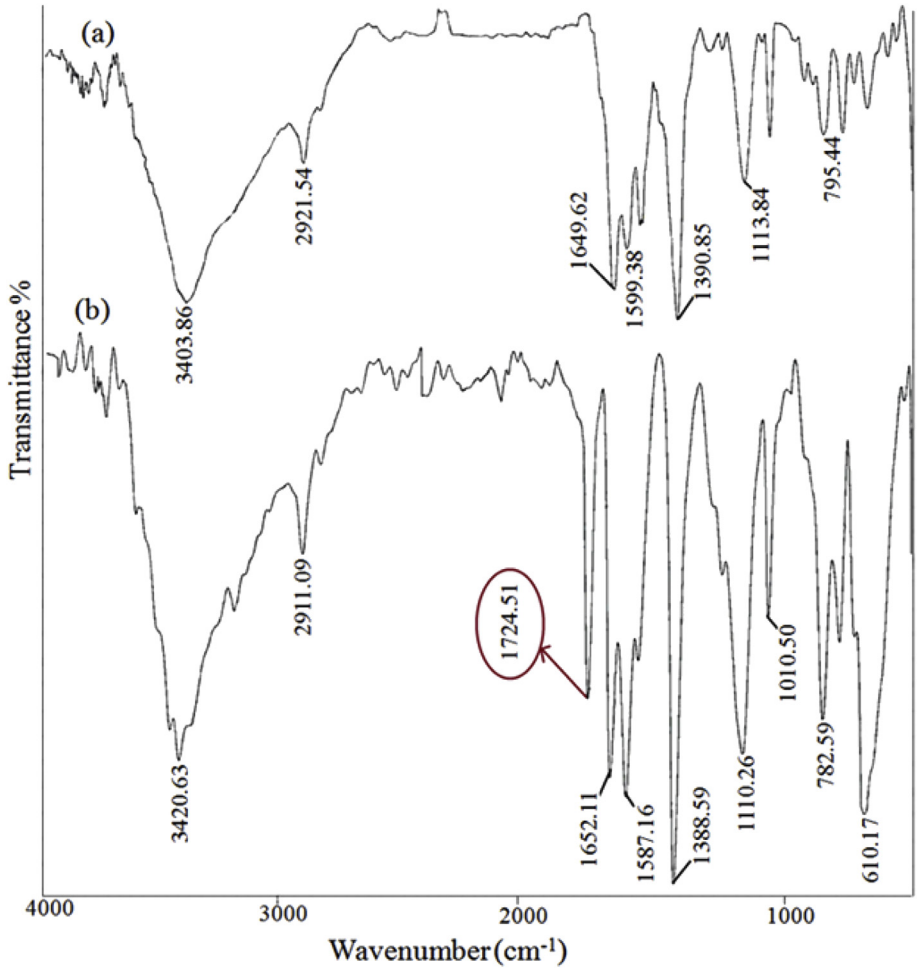

Fig. 2. FT-IR spectra of (a) Mn(TCPP)OAc and (b) Mn(TCPP)OAc@MWCNT.

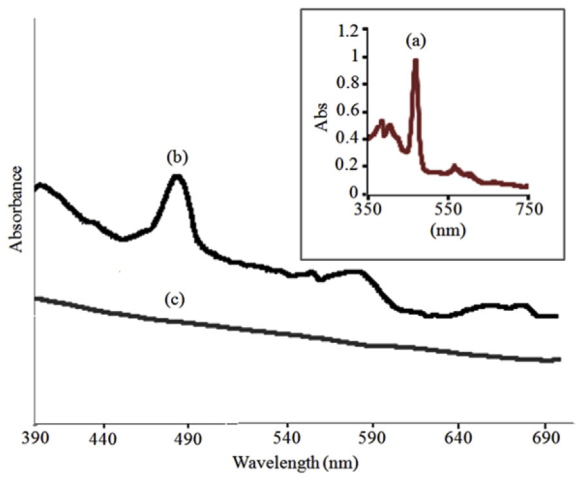

Fig. 3. UV–vis spectra of (a) Mn(TCPP)OAc, (b) Mn(TCPP)OAc@MWCNT and (c) MWCNT-OH.

13.6 mg imidazole enhanced the catalytic efficiency to 79%, and a decrease in catalytic efficiency was observed beyond 13.6 mg. Our results also show that the oxidation efficiency was affected by the amount of catalyst and oxidant (Table 1, entries 8 and 11–15). When the catalyst amount increased from 0.5 to 1 mg the catalytic efficiency increased by about 25% (from 54% to 79%), but with an increase in the amount of catalyst from 1 mg to 2 mg the catalytic efficiency improved by only 9% (from 79% to 88%). Another investigation was done on the oxidant concentration and the results show that when the oxidant amount was raised from 3×10^{-3} to 9×10^{-3} cm^3, the catalytic efficiency enhanced from 51% to 79% and beyond this concentration the catalytic efficiency improved by only 8% (from 79 to 87%). The oxidative degradation of the catalyst in higher amounts of catalyst and oxidant can be account for these observations. Thus, for checking other parameters such as reaction time, pH and temperature, 1 mg of catalyst and 9×10^{-3} cm^3 of the oxidant were chosen.

In order to determine the optimum reaction time, the catalytic reaction was also studied at various reaction times. The results show that the oxidative degradation

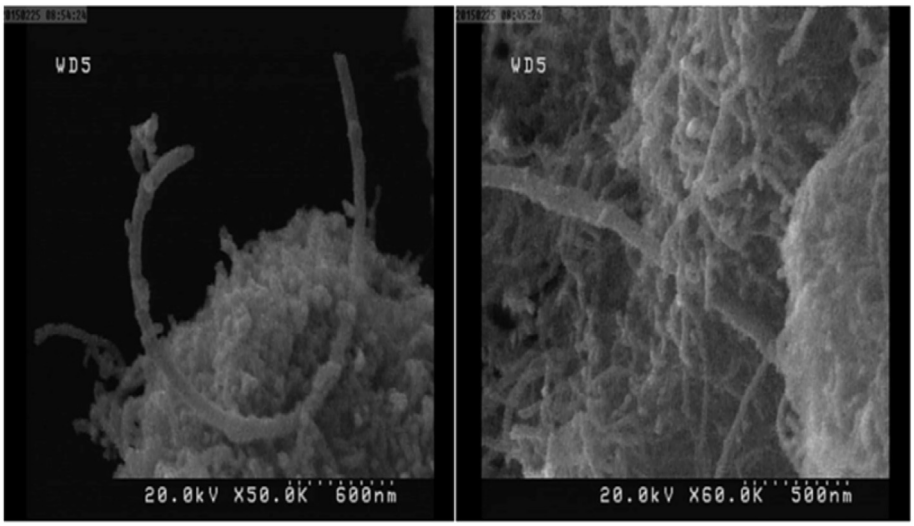

Fig. 4. FE-SEM images of the supported catalyst (Mn(TCPP)OAc@MWCNT) in two views.

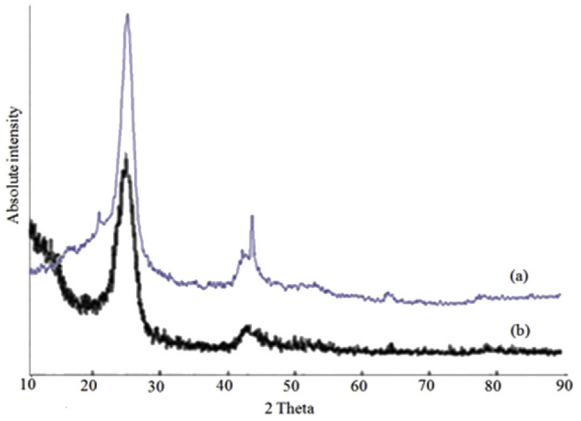

Fig. 5. XRD patterns of (a) Mn(TCPP)OAc@MWCNT and (b) MWCNT-OH.

proceeded sluggishly after 4 h. When the reaction time was increased from 4 h to 12 h, only a little increase in the catalytic efficiency was observed (about 10%) (Fig. 7).

Temperature is one of the most important factors in the catalytic reactions, especially in the catalytic processes utilized in environmental and industrial applications. Therefore, the impact of temperature on the performance of the supported catalyst was probed and the results are shown in Fig. 8. The oxidative degradation process was performed at 10, 40, 60 and 90 °C. In order to carry out more precise investigation, the reactions were run in the shorter reaction times (1 h and 2 h). When the temperature increased from 40 to 60 °C in 1 h, the degradation of MO increased from 66% to 85%. While at 90 °C, the degradation of MO reached 77%. Thus the best temperature for catalytic activity is 60 °C. At this temperature, the rate of oxidative degradation reached to 91% after 4 h.

Industrial wastes usually have various pH values and dye oxidation is strongly affected by varying the dye solution pH [46–48]. Thus, performance of a catalytic system over a wide range of pH is very important. So, an attempt was done to examine the effect of initial pH of the dye solution on the oxidative degradation of MO. The pH was adjusted at 5, 7, 9 and 11 using ammonium acetate buffer and experiments were run for 1 h. According to the results presented in the Figs. 9 and 10, catalytic efficiency of the supported catalyst was accelerated by enhancing the pH values. Presumably, the lower catalytic degradation of the MO under acidic conditions may be due to the dissociation of TBHP from the surface of the catalyst [49]. According to the literature studies [50,51] in the absence of the catalyst, MO is stable even in the presence of strong oxidants such as TBHP at low pH values and it can be oxidized by peroxides at high pH values but the reaction is very slow. In the presence of the Mn(TCPP)OAc@MWCNT as the catalyst, oxidation of MO can be performed over a wide range of pH from acidic to alkaline conditions in the shorter reaction time.

The UV–vis spectra of methyl orange before and after oxidation reaction are displayed in Fig. 11. Oxidative degradation of the dye causes a decrease in the peak at 464 nm which is attributed to the $n \rightarrow \pi^*$ transition.

The oxidative degradation products of the MO were monitored by HPLC-MS. Two pathways are proposed for oxidative cleavage of azo dyes: (i) asymmetrical and (ii) symmetrical. It is believed that both of these pathways occur during oxidative degradation reaction of azo dyes [52,53]. In the present study, the negative ion mode of MS analysis was employed and six main products were detected. *N*,*N*-dimethyl-*p*-phenylenediamine (*m*/*z* 136) and 4-aminobenzenesulfonate (*m*/*z* 172) were proposed for symmetrical azo bond cleavage and also benzenesulfonate (*m*/*z* 157), 4-(dimethylamino)-phenol (*m*/*z* 137), 4-carboxybenzenesulfonate (*m*/*z* 201) and 4-diazenyl-*N*,*N*-dimethylaniline (*m*/*z* 149) were proposed for asymmetrical azo bond cleavage. Two types of cleavage are presented in Fig. 12.

Performance of this catalytic system was also studied in the oxidation of the three other dyes: congo red (CR),

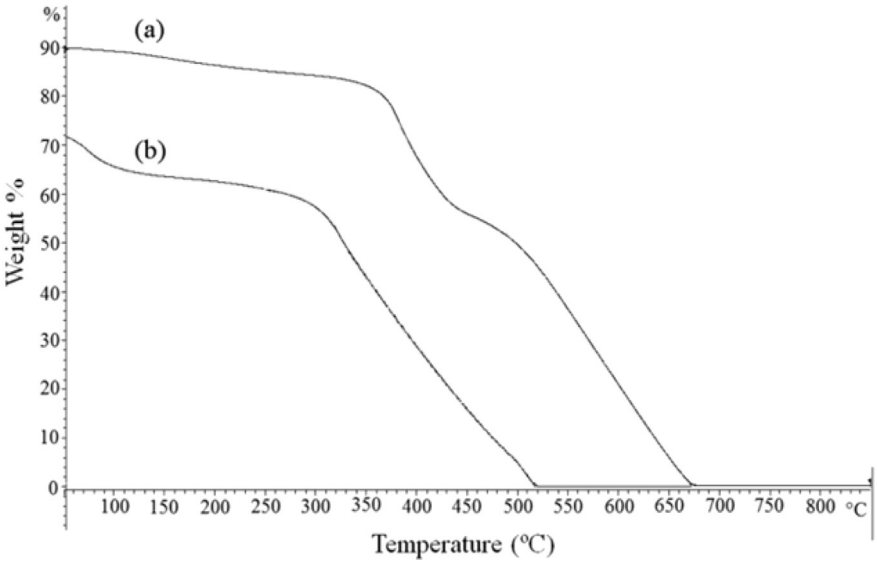

Fig. 6. TGA curves of (a) Mn(TCPP)OAc@MWCNT and (b) Mn(TCPP)OAc.

Table 1
The screening amount of the catalyst, oxidant and co-catalyst in the oxidation of MO using TBHP catalysed by using the supported catalyst (Mn(TCPP)OAc@MWCNT) at room temperature for 4 h.[a]

Entry	Catalyst amount (μmol)	Oxidant amount (mmol)	Co-catalyst amount (mg)	Oxidative degradation (%)
1	None	0.075	None	10
2	0.497	None	None	5
3	MWCNT-OH	None	None	13
4	0.497	0.075	None	11
5	0.497	0.075	3.4	43
6	0.497	0.075	6.8	58
7	0.497	0.075	10.2	75
8	0.497	0.075	13.6	79
9	0.497	0.075	20.4	78
10	0.497	0.075	54.4	71
11	0.248	0.075	13.6	54
12	0.994	0.075	13.6	88
13	0.497	0.025	13.6	51
14	0.497	0.050	13.6	67
15	0.497	0.125	13.6	87

[a] Reaction conditions: Molar ratio of the catalyst:TBHP is 1:150 and 3.3 cm^3 of 500 mg/dm^3 aqueous solution of MO. The initial reaction pH is 6.

methylene blue (MB) and crystal violet (CV) (Table 2). CR is a diazo dye and its UV–vis spectrum shows a maximum absorbance around 498 nm in aqueous solution. Control experiment was performed in the presence of the oxidant without the supported catalyst and only 4% of the absorbance peak at 498 nm was decreased after 4 h. In addition, the adsorption process of this dye was investigated in the presence of the supported catalyst without an oxidant and only 7% of the CR was adsorbed onto the surface of the supported catalyst after 4 h. In the presence of both the oxidant and supported catalyst, 74% oxidation of the CR occurred after 4 h (Table 2, entry 1) while in the pH = 11, 82% oxidation of the CR will be obtained (Table 2, entry 2). MB and CV show maximum absorbance around 660 and 590 nm, respectively.

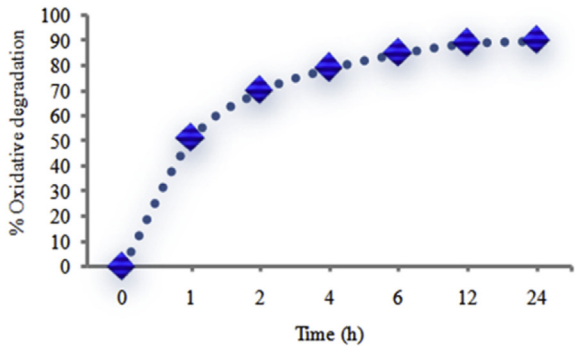

Fig. 7. Percentage of MO oxidative degradation as a function of time. Experimental conditions: 1 mg of catalyst, 9×10^{-3} cm^3 of TBHP, 3.3 cm^3 of 500 mg/dm^3 aqueous solution of MO and reactions were run at room temperature.

The results show that 10% or 25% of the MB or CV have been adsorbed onto the surface of the supported catalyst.

The results for oxidation of MB and CV with TBHP are presented in Table 2 (entries 3–6). The obtained results

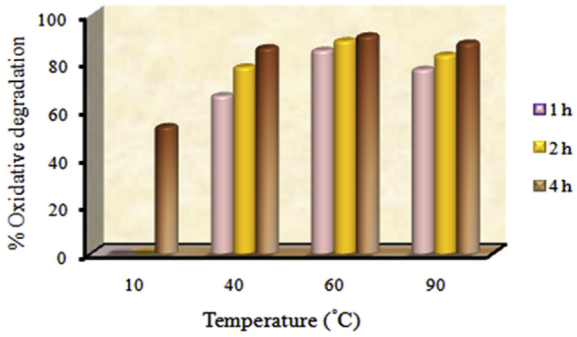

Fig. 8. Percentage of MO oxidative degradation as a function of temperature. Experimental conditions: 1 mg of catalyst, 9×10^{-3} cm^3 of TBHP, 3.3 cm^3 of 500 mg/dm^3 aqueous solution of MO.

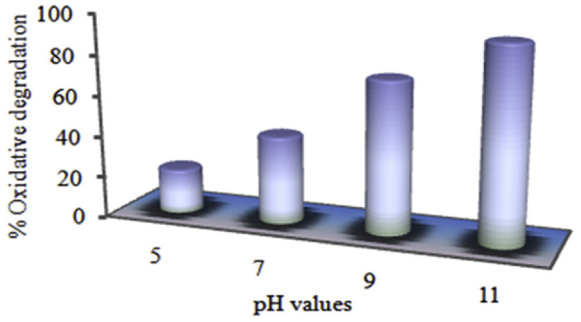

Fig. 9. The effect of pH values on the oxidative degradation of MO. Experimental conditions: 1 mg of catalyst, 9×10^{-3} cm^3 of TBHP, 3.3 cm^3 of 500 mg/dm^3 buffer solution of MO and reactions were run for 1 h.

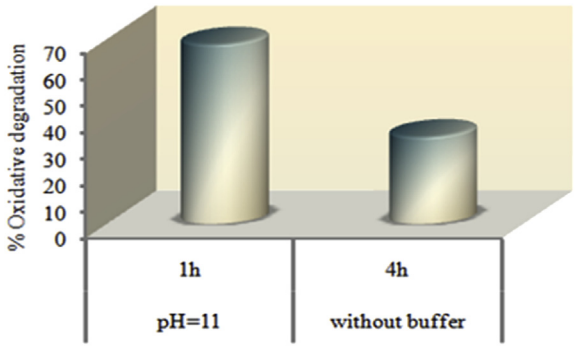

Fig. 10. Comparison of the catalytic activity of Mn(TCPP)OAc@MWCNT with or without buffer solution. Experimental conditions: 1 mg of catalyst, 9×10^{-3} cm^3 of TBHP, 6.5 cm^3 of 500 mg/dm^3 buffer solution of dye and reactions were run at room temperature.

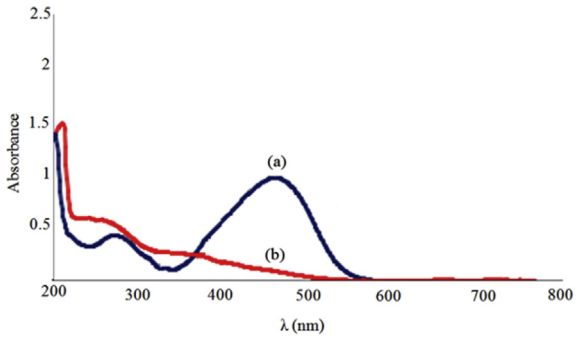

Fig. 11. UV–vis absorption spectra of the reaction mixture (a) before the oxidation reaction and (b) after the oxidation reaction in the presence of 1 mg of catalyst, 9×10^{-3} cm^3 of TBHP, and 3.3 cm^3 of 500 mg/dm^3 buffer solution of MO. The reactions were run for 1 h at pH = 11 at room temperature.

confirmed that Mn(TCPP)OAc@MWCNT is a suitable heterogeneous catalyst for oxidation of various dyes.

Comparison of this catalytic system with previously reported systems shows that higher dye degradation or lower reaction time was achieved [3,12,54].

3.3. Oxidation of 2,6-dimethylphenol

In addition to the oxidation of different synthetic textile dyes, the ability of the prepared heterogeneous catalyst to oxidize 2,6-dimethylphenol has been investigated (Fig. 13).

According to the results (Fig. 14), this catalytic system was also active in the oxidation of 2,6-dimethylphenol with high selectivity toward quinones. Control experiments show that the existence of the catalyst is essential (only 20% oxidation of 2,6-dimethylphenol will be achieved after 24 h in the absence of the catalyst). In the presence of the catalyst and oxidant, the efficiency of the catalyst increased with increasing the reaction time and the highest conversion (96%) was obtained after 5 h.

3.4. Proposed catalytic mechanism

In the proposed catalytic cycle, it seems that the oxidant can be coordinated to the metal center and compound I or/and II (Scheme 1) will be formed which can be used for oxidation of phenol or oxidative degradation of dyes [10,55]. The formation of quinone in the oxidation of phenols may be explained by two routes: (a) a radical mechanism initiated in the presence of the high valent metal oxo species [56–59] or (b) direct oxygenation from compound I analogue [60].

3.5. Catalyst stability

In order to study the stability and reusability of the supported catalyst, 2,6-dimethylphenol was selected as a model substrate. A series of sequential experiments were done in which the used catalyst was centrifuged, washed thoroughly with acetonitrile and methanol, dried at room temperature and then employed without any treatment in the next run (Fig. 15). Interestingly, the catalyst maintains a considerable part of its catalytic efficiency after reusing several times and reaches to about 56% after the sixth reaction. Hence, this catalyst can be considered as an excellent option for industrial applications.

4. Conclusions

In this research, a simple heterogeneous catalyst was prepared through covalent bonding between Mn-porphyrin and multi-walled carbon nanotubes. This heterogeneous catalyst exhibits efficient catalytic activity in the oxidative degradation of synthetic textile dyes, in aqueous solution over a wide range of pH at ambient temperature using TBHP. By using HPLC-MS analysis, six main products were detected and two main pathways were proposed for oxidative degradation of MO. On the other hand, this simple supported catalyst was successfully able to perform the selective and efficient oxidation of 2,6-dimethylphenol as a phenolic substrate toward quinones under mild conditions. Furthermore, this catalyst can be recovered and reused several times and according to the results, this catalytic system can be suitable for a potential industrial application.

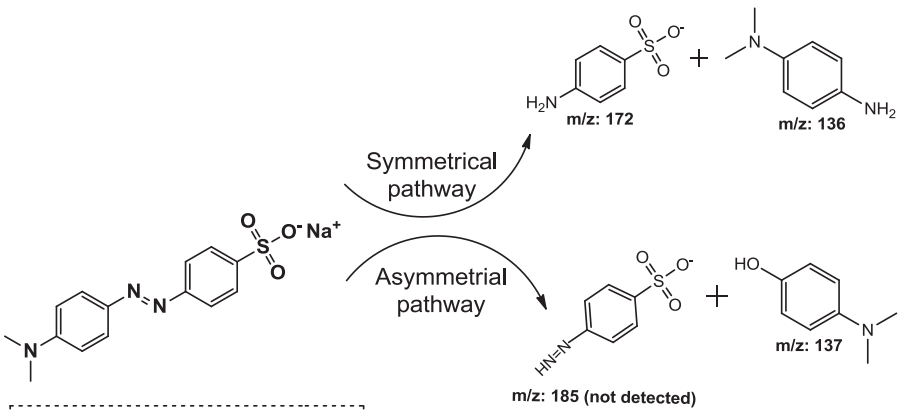

Products	m/z
N,N-dimethyl-*p*-phenylenediamine	136
4-(dimethylamino)-phenol	137
4-diazenyl-N,N-dimethylaniline	149
benzenesulfonate	157
4-aminobenzenesulfonate	172
4-carboxybenzenesulfonate	201

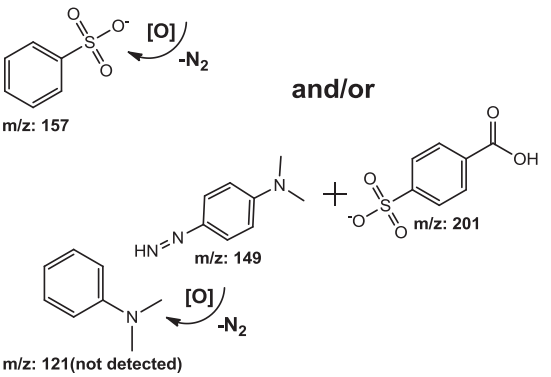

Fig. 12. Possible pathways for oxidative cleavage of MO using TBHP catalysed by Mn(TCPP)OAc@MWCNT.

Table 2
The monitoring of the oxidation of the three other dyes using TBHP catalysed by Mn(TCPP)OAc@MWCNT at room temperature.

Entry	Dye	pH	Time (h)	Oxidative degradation (%)
1	Congo red	Without buffer	4	74
2	Congo red	11	1	82
3	Methylene blue	Without buffer	4	69
4	Methylene blue	11	1	90
5	Crystal violet	Without buffer	4	73
6	Crystal violet[a]	11	–	–

[a] Crystal violet is insoluble at pH = 11.

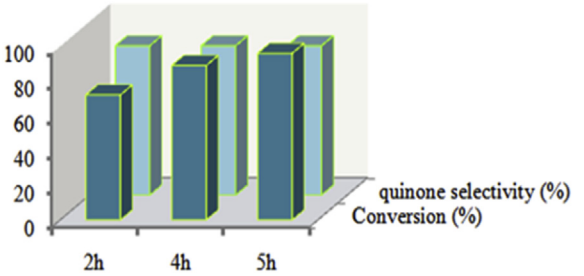

Fig. 14. Oxidation of 2,6-dimethylphenol using TBHP catalysed by Mn(TCPP)OAc@MWCNT at room temperature. The molar ratio of catalyst: co-catalyst: substrate: oxidant is 1:20:50:150 in acetonitrile (0.5 mL).

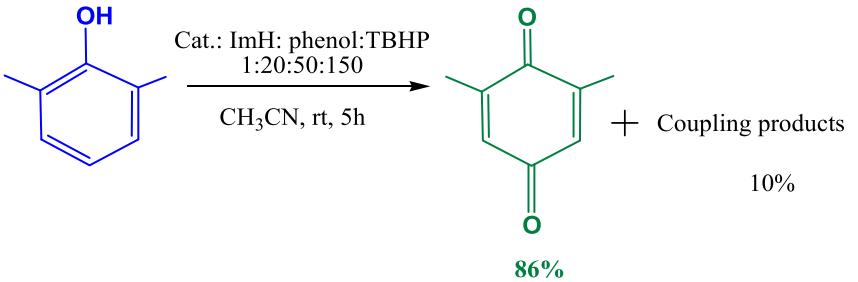

Fig. 13. Oxidation of 2,6-dimethylphenol.

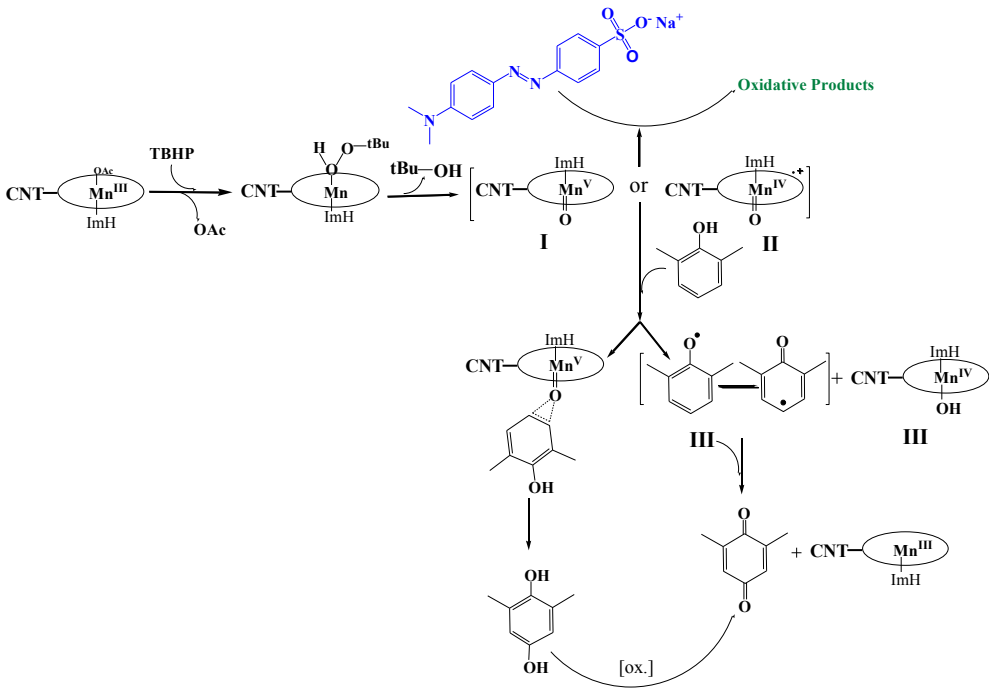

Scheme 1. Proposed mechanism for oxidation of dye and 2,6-dimethylphenol.

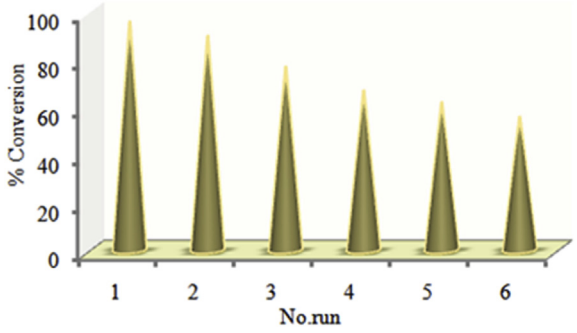

Fig. 15. Reusability of the supported catalyst, Mn(TCPP)OAc@MWCNT, in the oxidation of 2,6-dimethylphenol using TBHP at room temperature.

Acknowledgements

Financial support of this work by K.N. Toosi University of Technology is gratefully acknowledged.

References

[1] M. Dakiky, I. Nemcova, Dyes Pigments 44 (2000) 181.
[2] C. Sahoo, A.K. Gupta, A. Pal, Dyes Pigments 66 (2005) 189.
[3] R. Aravindhan, N.N. Fathima, J.R. Rao, B.U. Nair, J. Hazard. Mater. B 138 (2006) 152.
[4] W. Chen, W. Lu, Y. Yao, A. Xu, Environ. Sci. Technol. 41 (2007) 6240.
[5] R. Nishimoto, Q. Zhu, T. Miyamoto, T. Sato, X. Tu, A. Aneksampant, M. Fukushima, J. Mol. Catal. A: Chem. 396 (2015) 84.
[6] M.T. Hassanein, S.S. Gerges, M.A. Abdo, S.H. El-Khalafy, J. Porph. Phthal. 9 (2005) 621.
[7] B. Meunier, A. Sorokin, Acc. Chem. Res. 30 (1997) 470.
[8] P. Zucca, A. Rescigno, M. Pintus, A.C. Rinaldi, E. Sanjust, Chem. Cent. J. 6 (2012) 161.
[9] T.K. Saha, H. Frauendorf, M. John, S. Dechert, F. Meyer, ChemCatChem 5 (2013) 796.
[10] P. Zucca, C. Vinci, A. Rescigno, E. Dumitriu, E. Sanjust, J. Mol. Catal. A: Chem. 321 (2010) 27.
[11] V.P. Barros, M.D. Assis, J. Braz. Chem. Soc. 24 (2013) 830.
[12] V.P. Barros, A.L. Faria, T.C.O. MacLeod, L.A.B. Moraes, M.D. Assis, Int. Biodeter. Biodeger. 61 (2008) 337.
[13] P. Zucca, G. Cocco, S. Manca, D. Steri, E. Sanjust, J. Mol. Catal. A: Chem. 394 (2014) 129.
[14] S. Rayati, P. Abdolalian, Appl. Catal. A: Gen. 456 (2013) 240.
[15] S. Zakavi, T.M. Yazdeli, J. Mol. Catal. A. Chem. 367 (2013) 108.
[16] N. Safari, S. Rayati, A. Ghaemi, F. Bahadoran, H.R. Khavasi, Inorg. Chem. Commun. 11 (2008) 1459.
[17] M.M.Q. Simões, C.M.B. Neves, S.M.G. Pires, M.G.P.M.S. Neves, J.A.S. Cavaleiro, Pure Appl. Chem. 85 (2013) 1671.
[18] P. Zucca, A. Rescigno, A.C. Rinaldi, E. Sanjust, J. Mol. Catal. A: Chem. 388–389 (2014) 2.
[19] L.B. Bolzon, H.R. Airoldi, F.B. Zanardi, J.G. Granado, Y. Iamamoto, Micropor. Mesopor. Mater. 168 (2013) 37.
[20] B.T. Holland, C. Walkup, A. Stein, J. Phys. Chem. B 102 (1998) 4301.
[21] A.K. Rahiman, K. Rajesh, K.S. Bharathi, S. Sreedaran, V. Narayanan, Appl. Catal. A. Gen. 314 (2006) 216.
[22] T. Schilling, A. Okunola, J. Masa, W. Schuhmann, M. Bron, Electrochim. Acta 55 (2010) 7597.
[23] D. Tasis, N. Tagmatarchis, A. Bianco, M. Prato, Chem. Rev. 106 (2006) 1105.
[24] H. Chu, L. Wei, R. Cui, J. Wang, Y. Li, Coord. Chem. Rev. 254 (2010) 1117.
[25] S. Rayati, E. Bohloulbandi, C. R. Chimie 17 (2014) 62.
[26] S. Rayati, P. Jafarzadeh, S. Zakavi, Inorg. Chem. Commun. 29 (2013) 40.
[27] S. Rayati, S. Zakavi, P. Jafarzadeh, O. Sadeghi, M.M. Amini, J. Porph. Phthal. 16 (2012) 260.
[28] S. Rayati, Z. Sheybanifard, J. Porph. Phthal. 19 (2015) 622.
[29] S. Nishibe, H. Kinoshita, H. Takeda, G. Okano, Chem. Pharm. Bull. 38 (1990) 1763.
[30] A.M. Sastre, A. Madi, F.J. Alguacil, J. Membr. Sci. 166 (2000) 213.
[31] A.B. Sorokin, S. Mangematin, C. Pergrale, J. Mol. Catal. A: Chem. 182–183 (2002) 267.
[32] M.A. El-Sayed, H.A. El-Wakil, T.S. Kassem, H.A. Abo-Eldahab, A.E. El-Kholy, Inorg. Chim. Acta 359 (2006) 4304.
[33] P. Villabrille, G. Romanelli, P. Vázquez, C. Cáceres, Appl. Catal. A. Gen. 270 (2004) 101.

[34] A.D. Adler, F.R. Longo, W. Shergalis, J. Am. Chem. Soc. 86 (1964) 3145.
[35] J.W. Buchler, G. Eikellmann, J. Puppe, K. Rohback, H. Schneehage, D. Weck, Justus. Liebigs. Ann. Chem. 745 (1971) 135.
[36] S. Balalaie, M. Mahdidust, R.E. Najafabadi, Chin. J. Chem. 26 (2008) 1141.
[37] A. Rezaeifard, M. Jafarpour, Catal. Sci. Technol. 4 (2014) 1960.
[38] C. Crestini, A. Pastorini, P. Tagliatesta, J. Mol. Catal. A: Chem. 208 (2004) 195.
[39] G.S. Machado, K.A.D.F. Castro, F. Wypych, S. Nakagaki, J. Mol. Catal. A: Chem. 283 (2008) 99.
[40] M. Halma, A. Bail, F. Wypych, S. Nakagaki, J. Mol. Catal. A: Chem. 243 (2006) 44.
[41] F. Esnaashari, M. Moghadam, V. Mirkhani, S. Tangestaninejad, I. Mohammadpoor-Baltork, A.R. Khosoropour, M. Zakeri, S. Hushmandrad, Polyhedron 48 (2012) 212.
[42] T. Belin, F. Epron, Mater. Sci. Eng. B 119 (2005) 105.
[43] N. Panda, H. Sahoo, S. Mohapatra, J. Hazard. Mater. 185 (2011) 359.
[44] A.C. Serra, C. Docal, A.R. Gonsalves, J. Mol. Catal. A: Chem. 238 (2005) 192.
[45] J. Tokuda, R. Ohura, T. Iwasaki, Y. Takeuchi, A. Kashiwada, M. Nango, Textile. Res. J. 69 (1999) 956.
[46] K. László, E. Tombácz, C. Novák, Colloid. Surf. A. 306 (2007) 95.
[47] Y. Arcand, J. Hawari, S.R. Guiot, Water. Res. 29 (1995) 131.
[48] W. Lu, W. Chen, N. Li, M. Xu, Y. Yao, Appl. Catal. B. Environ. 87 (2009) 146.
[49] W. Lu, N. Li, W. Chen, Y. Yao, Carbon 47 (2009) 3334.
[50] J. Oakes, P. Gratton, J. Chem. Soc., Perkin Trans. 2 (1998) 2563.
[51] A.S. Makarova, E.V. Kudrik, S.V. Makarov, O.I. Koifman, J. Porph. Phthal. 18 (2014) 604.
[52] J. Zhang, M. Feng, Y. Jiang, M. Hu, S. Li, Q. Zhai, Chem. Eng. J. 191 (2012) 236.
[53] F. Luo, D. Yang, Z. Chen, M. Megharaj, R. Naidu, J. Hazard. Mater. 296 (2015) 37.
[54] F.R. Araújo, J.G. Baptista, L. Marcal, K.J. Ciuffi, E.J. Nassar, P.S. Calefi, M.A. Vicente, R. Trujillano, V. Rives, A. Gil, S. Korili, E.H. de Faria, Catal. Today 227 (2014) 105.
[55] J.T. Groves, M.K. Stern, J. Am. Chem. Soc. 110 (1988) 8628.
[56] A. Sorokin, B. Meunier, Chem. Eur. J. 2 (1996) 1308.
[57] N.W.J. Kamp, J.R.L. Smith, J. Mol. Catal. A: Chem. 113 (1996) 131.
[58] N. Colclough, J.R.L. Smith, J. Chem. Soc., Perkin. Trans. 2 (1994) 1139.
[59] G.R. Hodges, J.R.L. Smith, J. Oakes, J. Chem. Soc., Perkin Trans. 2 (1999) 1943.
[60] W. Adam, W.A. Herrmann, J. Lin, C.R. Saha-Möller, J. Org. Chem. 59 (1994) 8281.